crystals

MDPI

Communication

Crystal Structure of the Biocide Methylisothiazolinone

Richard Goddard [1], Rüdiger W. Seidel [2], Michael Patzer [1] and Nils Nöthling [1,*]

[1] Max-Planck-Institut für Kohlenforschung, Kaiser-Wilhelm-Platz 1, 45470 Mülheim an der Ruhr, Germany; goddard@mpi-muelheim.mpg.de (R.G.); patzer@mpi-muelheim.mpg.de (M.P.)
[2] Institut für Pharmazie, Martin-Luther-Universität Halle-Wittenberg, Wolfgang-Langenbeck-Straße 4, 06120 Halle (Saale), Germany; ruediger.seidel@rub.de
* Correspondence: noethling@mpi-muelheim.mpg.de; Tel.: +49-208-306-2170

Abstract: Methylisothiazolinone (MIT) is widely used as a biocide in numerous personal care products, glass-cleaning liquids, paints, and industrial applications. MIT and related isothiazolinones have attracted much attention for their allergenic properties such as contact dermatitis. Although the compound was first prepared in 1964 and has been widely used as a biocide since the 1970s, its crystal structure has so far not been reported. Here we report the solid state structure of MIT as determined by single crystal X-ray diffraction (SC-XRD) analysis of a crystal grown from the melt. MIT crystallizes as a layered structure with short C-H···O hydrogen bonding interactions within the sheets. The average distance between the sheets parallel to (1 0 2) is ca. 3.2 Å. The molecule exhibits a small C-S-N angle of 90.81(2)° and a methyl group that is slightly bent out of the plane of the planar five-membered ring. The sulfur atom does not undergo any significant intermolecular interactions.

Keywords: methylisothiazolinone; biocide; crystal structure analysis; hydrogen bonding; Hirshfeld analysis; melt crystallization

Citation: Goddard, R.; Seidel, R.W.; Patzer, M.; Nöthling, N. Crystal Structure of the Biocide Methylisothiazolinone. *Crystals* **2024**, *14*, 1100. https://doi.org/10.3390/cryst14121100

Academic Editor: Alexander Y. Nazarenko

Received: 19 November 2024
Revised: 15 December 2024
Accepted: 17 December 2024
Published: 20 December 2024

1. Introduction

Methylisothiazolinone (MIT; systematic name: 2-methyl-1,2-thiazol-3(2*H*)-one) (Scheme 1) is a widely used biocide often used together with 5-chloro-2-methyl-1,2-thiazol-3(2*H*)-one (MCI) [1]. MIT is active against Gram-positive and Gram-negative bacteria, as well as fungi, when used in combination with methylchloroisothiazolinone (MCI) with reported minimum inhibitory concentration values of 0.0002, 0.0002, 0.00005, and 0.00005% (*w*/*w*) for *Staphylococcus aureaus*, *Pseudomonas aeruginosa*, *Aspergillus niger*, and *Candida albicans*, respectively [2]. Its biological activity is thought to arise from its ability to initially diffuse through the membranes of bacteria or fungal cell walls and then react with important intracellular sulfur-containing proteins, or simpler thiols inside the cell, causing the cell function to be impaired [3]. Isothiazolinones and 5-chloroisothiazolinones react chemoselectively with thiols by cleavage of the weak nitrogen–sulfur bond to form disulfides. They show selectivity for inhibition of the thiol-dependent cysteine protease cathepsin B and the histone acetyltransferase p300/CBP associated factor (PCAF) based on their substitution pattern [4]. Growth inhibitory activity against *Escherichia coli* ATCC 8739 and *Schizosaccharomyces plombe* NCYC 1534 is rapidly quenched by the addition of thiol containing materials such as glutathione and cysteine, and the non-thiol amino acids valine or histidine [3].

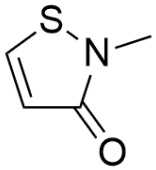

Scheme 1. Structural formula of 2-methyl-2*H*-isothiazol-3-one (MIT).

MIT is prepared by cyclization of *cis*-*N*-methyl-3-thiocyanoacrylamide, which was conveniently prepared from its precursor *N*-methylpropiolamide, with a reported overall yield of 80%, and forms an equilibrium with *cis*-3-thiocyanoacrylamide [5]. A number of protocols can be found in the literature describing the synthesis of MIT and MCI [6]. The compound can be stabilized by magnesium and other salts and is commercially sold as Laxness Kathon among other products [7]. According to a Swiss study, 43% of paints, varnishes and coatings in Switzerland in 2000 contained the mixture MCI/MIT [8]. The figure for adhesives, fillers, and sealants was 45%. MIT shows reactivity towards nucleophiles and the cLogP = −0.11 indicates that MIT is hydrophilic [9]. It can penetrate the skin [10,11]. Proton NMR spectra reveal that MIT reacts with cysteine to yield a single reaction product together with some residual unreacted cysteine [3]. MIT and isothiazolinones, in general, have been associated with allergic reactions of the skin [12] but there is some evidence that symptoms can be avoided by prior application of glutathione [13,14].

Although MIT was first prepared in 1964 [15] based on a previously reported rearrangement of a 1,4-thiazepine ring and formation of 3-isothiazolinones [16], its crystal structure has not been reported hitherto as far as we are aware. Since the compound has a solubility of greater than 1000 g/L in water [17], a low melting point of 50–51 °C [5,10,15,18] and does not decompose on melting, we decided to grow a crystal suitable for crystal structure analysis from the melt in a glass capillary. Here, we describe the preparation of the crystal and the results of the crystal structure analysis, which reveals short intermolecular C-H···O hydrogen bonds in the crystal and no close S···S contacts.

2. Materials and Methods

2.1. In Situ Cryocrystallization

The title compound was purchased from Sigma Aldrich, Schnelldorf, Germany (95% purity) and used as received. After initial DSC studies and the measurement of an ATR-FT-IR spectrum (see Supporting Information), which indicated the presence of water in the sample (see Figures S1, S2 and S6), ca. 50 mg of the solid was melted by using a hot air blower and transferred into a heated borosilicate glass capillary with a diameter of 0.5 mm (WJM-Glas Müller GmbH, Berlin, Germany) mounted on a magnetic base (Hampton Research, Aliso Viejo, CA, USA). The base with the capillary was then placed on the goniometer head of the single-crystal X-ray diffractometer, in the nitrogen gas stream from an Oxford Instruments cryostat maintained at 325 K. The sample was first cooled to 200 K in order to induce crystallization. The polycrystalline powder was then partially melted by moving the capillary in and out of the cold gas stream, while retaining some solid in the capillary, until the tube was filled with a single crystal. The capillary was then rapidly cooled down to 100 K for the collection of the diffraction data.

2.2. X-Ray Intensity Data Collection and Processing

The diffraction data were collected from the sample maintained at 100 K by a cold nitrogen gas stream on a Bruker AXS Kappa Mach3 diffractometer, equipped with an Incoatec IμS microfocus Mo K_α X-ray source, Incoatec multilayer optics and an Apex II CCD detector. The data collection involving both φ and ω scans was controlled with APEX4 (Bruker AXS, Karlsruhe, Germany), and the raw diffraction data were processed with SAINT (Bruker AXS, Karlsruhe, Germany). An absorption correction, using the Gaussian method based on indexed crystal faces, was carried out with SADABS-2016/2 (Bruker AXS, Karlsruhe, Germany).

2.3. Structure Solution and Refinement

The crystal structure was solved with SHELXT [19] and initially refined with SHELXL-2019/3 [20]. The final structure refinement was conducted using NoSpherA2 [21,22] in Olex2 [23] with Hirshfeld partitioning of the electron density calculated in ORCA 5.0 [24] (B3LYP [25,26]/def2-TZVPP [27]). Anisotropic atomic displacement parameters were introduced for all atoms. In addition, the sulfur atom was allowed to refine anharmonically

using a Gram Charlier expansion to fourth order implemented in Olex2. This resulted in a decrease in R_1 from 0.028 to 0.024 and a reduction in the average standard uncertainty of the bond distances by 4%, despite the additional 25 parameters associated with theanharmonic refinement. The structure refinement converged with a data-to-parameter ratio of 30.2, with intensity data measured to a resolution of 0.53 Å. Structure pictures were drawn with Mercury [28]. Table 1 lists crystal data and refinement details for MIT.

Table 1. Crystal data and refinement details for MIT.

empirical formula	C_4H_5NOS
M_r	115.157
T (K)	100(2)
λ (Å)	0.71073
crystal system	triclinic
space group	P-1
a (Å)	5.6037(6)
b (Å)	6.4473(7)
c (Å)	7.6391(9)
α (°)	67.857(2)
β (°)	77.541(3)
γ (°)	84.523(2)
V (Å^3)	249.59(5)
Z	2
p_{calc} (mg m^{-3})	1.532
μ (mm^{-1})	0.507
F(000)	120.313
crystal size (mm)	0.51 × 0.44 × 0.30
θ range for data collection (°)	2.94–41.67
reflections collected/unique	17,950/3288
R_{int}	0.0391
observed reflections [$I > 2\sigma(I)$]	2786
data/restraints/parameters	3288/0/134
goodness-of-fit on F^2	1.1698
$R1$ [$I > 2\sigma(I)$]	0.0244
$wR2$ (all data)	0.0598
Δp_{max}, Δp_{min} (e Å^{-3})	0.383, −0.247

2.4. Computational Methods

Hirshfeld surface analysis was performed with CrystalExplorer [29]. Density functional (DFT) calculations on the free molecule of MIT were performed starting from the molecular structure in the crystal using ORCA (version 6.0) [24] with a B3LYP/G (VWN1) hybrid functional (20% HF exchange) [25,26,30] and a def2-TZVPP basis set [27] with an auxiliary def2/J basis [31]. The optimization of the structure used the BFGS method from an initial Hessian according to Almlöf's model with a very tight self-consistent field convergence threshold [32]. The optimized local minimum-energy structure exhibited only positive modes. The structure picture was generated with Mercury [28]. Cartesian coordinates of the DFT-optimized structure of MIT can be found in the Supplementary Materials. Theoretical calculations for the molecular crystal were carried out using the CRYSTAL17 program [33,34]. The calculations were based on Kohn–Sham density functional theory [35]. The PBE exchange correlation functional was used [36]. For the treatment of dispersion interactions, the dispersion correction D3(BJ) was used [37–39]. The Weigend and Ahlrichs' def2-TZVP basis set stored in the program was used [27]. The SHRINK factor was set to 8. The fractional coordinates of the atoms were optimized to calculate the equilibrium geometry. The cell parameters were fixed to the values obtained in the experiment.

3. Results and Discussion

The results of the crystal structure analysis of MIT is summarized in Figure 1, which shows the atom numbering scheme and the contents of the triclinic unit cell, and Tables 2 and 3, which give selected distances and angles in the molecule and in the crystal. The C-S-N angle at 90.80(3)° is ca. 12° smaller than the corresponding angle in acyclic sulfenamides in the Cambridge Structural Database [40] (average of 102(2)° for 165 entries, see Figure S5) and reflects the influence of the five-membered ring. This compares with an average value of 89.6° in the structures of MCI [4,41–43] and 90.4° (average) in that of benzisothiazolinone (BIT) [44]. The S1-C5 distance of 1.7096(6) Å is shorter than the corresponding distance in BIT (average 1.74 Å), as is the S1-N2 distance (1.6851(5) Å), but both distances are comparable to those observed in the crystal structures of MCI. The relatively short C3-C4 bond distance of 1.4533(7) Å indicates that there is some conjugation of the double bonds in the C=C-C=O unit.

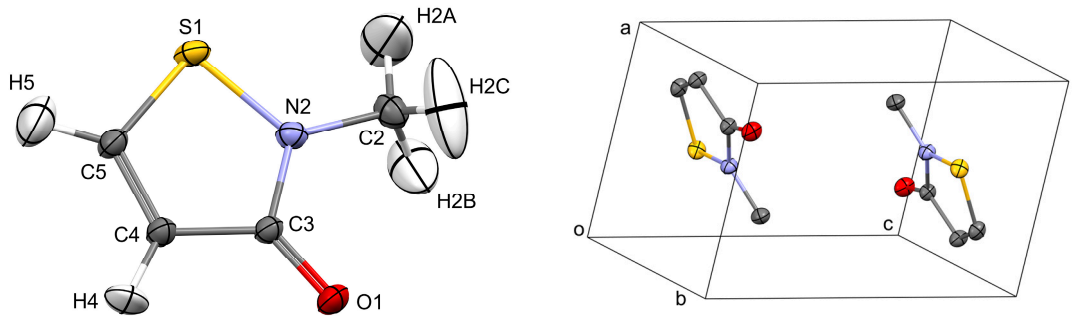

(**a**) (**b**)

Figure 1. (**a**) Molecular structure of MIT in the crystal. Displacement ellipsoids are drawn at the 50% probability level. (**b**) Packing of the two molecules of MIT in the triclinic unit cell. Hydrogen atoms are omitted for clarity. o, a, b, and c, denote the origin and unit cell axes, respectively.

Table 2. Selected distances (Å) and angles (°) in the structure of MIT.

Distance		Angle	
S1-N2	1.6851(5)	N2-S1-C5	90.81(2)
S1-C5	1.7096(6)	C3-C4-C5	112.68(4)
C4-C5	1.3509(7)	C4-C3-N2	108.79(4)
C3-C4	1.4533(7)	S1-N2-C3	114.93(4)
C3-O1	1.2373(6)	S1-N2-C4	122.41(4)
C3-N2	1.3734(6)	C2-N2-C4	122.34(4)
C2-N2	1.4508(7)	N2-C3-O1	122.59(4)
C-$H_{average}$	1.06(1)	C4-C3-O1	128.61(4)

Table 3. Selected hydrogen bond distances (Å) less than 3.5 Å and angles (°) in MIT.

Interaction	C-H	H···O	C···O	Angle
C5-H5···O1 [1]	1.056(10)	2.163(11)	2.9635(7)	130.9(8)
C4-H4···O1 [2]	1.077(9)	2.437(9)	3.4733(7)	160.9(9)

[1] [x, 1 + y, z]. [2] [−x, 1 − y, 2 − z].

The unit cell has a volume of 249.59(5) A^3 and is densely packed with a packing index according to Kitaigorodsky [45] of 73.75%. The molecular volume calculated on the basis of the cell volume is thus 124.8 $Å^3$. The packing of the molecules in the unit cell is notable. In contrast to the structures of MCI and BIT, which are packed with herring-bone type arrangements of molecules, the structure of MIT is characterized by a layered structure. Figure 2a,b show views perpendicular to the layers and the arrangement of molecules

in the individual sheets. The nearest Miller indices to the mean plane through the non-hydrogen atoms are (8 −1 19) or approximately (1 0 2). The distances between the mean planes of the molecules are 3.173 Å and 3.412 Å. Notably, the crystal is pure MIT, even though preliminary DSC studies and an ATR-FT-IR spectrum (see Supporting Information) indicated the presence of water in the sample used for the melt crystallization.

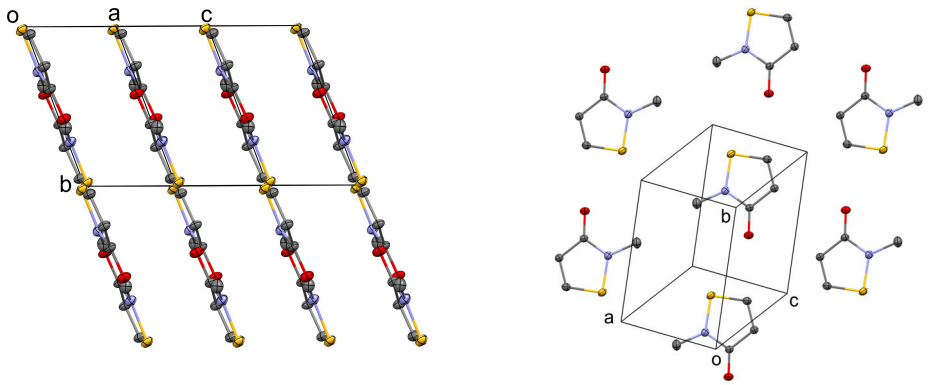

(**a**) (**b**)

Figure 2. (**a**) Depiction of the layered arrangement of the molecules in the crystal of MIT. (**b**) View approximately perpendicular to the sheet highlighting the close packing of the molecules. Hydrogen atoms have been omitted for clarity. 0, a, b, and c, denote the origin and unit cell axes, respectively.

The molecules appear to be held in position by C-H···O hydrogen bonds as revealed by the Hirshfeld surface and corresponding fingerprint plot in Figures 3a and 3b, respectively. The shortest and most likely strongest interaction is between the C-H group adjacent to the sulfur atom and the oxygen atom of a neighboring molecule. The C5-H5···O1[x, 1 + y, z] distance is short for a C-H···O hydrogen bonding interaction (C5···O1[x, 1 + y, z] 2.9635(7) Å) and links the molecules in chains. Pairwise, somewhat longer [C4···O1[−x, 1 − y, 2 − z] 3.4733(7) Å] but more linear [C4-H4···O1[−x, 1 − y, 2 − z] 160.9(9)°] C-H···O intermolecular hydrogen bonds about centers of symmetry in the crystal link the chains. A representation of the energy framework diagrams calculated with CrystalExplorer [29] is shown in Figure S8. Accordingly, the major interaction between the layers is dispersive in nature with the strongest dispersive interaction between adjacent molecules in neighboring sheets calculated to be −24.2 kJ/mol. Within the sheets the major interaction appears to be mainly electrostatic with the largest calculated total electrostatic interaction energy of −24.6 kJ/mol along the *b* axis direction. The C-H group attached to the sulfur atom is absent in the structure of MCI because of the chloro substituent but the remaining C-H group makes a somewhat shorter C-H···O hydrogen bond to the oxygen atom of a neighboring molecule and this results in a herring bone type of packing. BIT has no C-H groups but rather a N-H group which can undergo a classical N-H···O hydrogen bonding interaction in the crystal. Interestingly, the sulfur atom does not appear to undergo any significant intermolecular interactions in the crystal of MIT.

To see whether the packing had an effect on the geometry of the molecule of MIT, the structure of the free molecule was optimized using DFT calculations. Figure 4 shows a superposition of the molecule of MIT in the crystal structure with that of the calculated free molecule at the C-S-N unit. For comparison, the molecule of MCI in its crystal structure (CSD refcode: XIFRIO) is included. The root-mean-square fit between the non-hydrogen atoms of the isothiazolinone unit of MIT in the crystal and the optimized structure of the free molecule is 0.016 Å. The methyl group is found to lie slightly out of the plane. This is also the case for MCI but more so. It is noticeable that one of the methyl hydrogen atoms in the free molecule lies in the plane together with the adjacent C=O group, whereas this is not the case in the crystals of MIT and MCI. Instead, in MIT two of the hydrogen atoms point towards oxygen atoms in neighboring sheets. A solid-state DFT optimization of the structures of MIT and MCI using the experimental unit cell parameters resulted in a

O-C-N-C torsion angle of 3.5 ° (expt. 4.4 °) for MIT and −11.1 ° (expt. −10.9 °) for MCI (CSD Refcode: XIFRIO) [33,34].

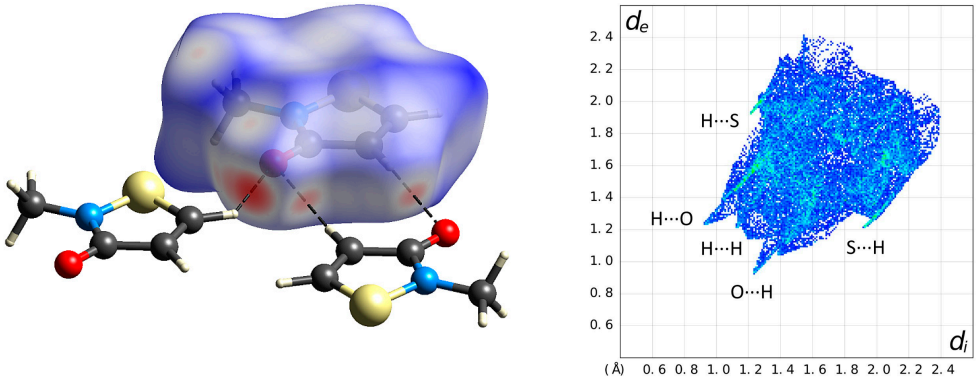

(**a**) (**b**)

Figure 3. (**a**) Hirshfeld surface mapped with d_{norm} showing the major intermolecular interactions within the crystalline structure of MIT; (**b**) 2D fingerprint plot of the Hirshfeld surface providing an overview of the intermolecular interactions.

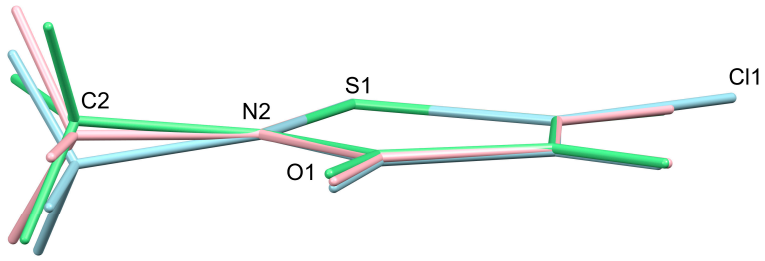

Figure 4. Superposition of the N-S-C units of the experimentally determined geometry of MIT (green) with those of the DFT optimized structure of the free molecule (pink) and MCI in the crystal structure (blue, CSD refcode: XIFRIO), illustrating the non-planarity of the nitrogen atom in the crystal structures of MIT and MCI and the different arrangements of the methyl hydrogen atoms.

4. Conclusions

The crystal structure analysis of MIT reveals a layered structure aligned approximately along (1 0 2) formed as a result of short intermolecular hydrogen bonding contacts in the sheets. The average distance between the sheets is ca. 3.2 Å. Based on the unit cell volume, the molecular volume is estimated to be 124.8 Å^3. The N-S-C angle at 90.80(3)° is remarkably small, but larger than the same angle in the more active but less soluble MCI (89.7°). The sulfur atom undergoes no significant intermolecular interactions in the crystal. Melt crystallization was successfully applied to determine the solid state structure of MIT for the first time. Crystallization from the melt provides an attractive alternative to recrystallization from solution, particularly when the compound is very soluble. We hope to apply this technique in the future to obtain structural information about unknown compounds that are difficult to crystallize using conventional methods.

Supplementary Materials: The following supporting information can be downloaded at: https://www.mdpi.com/article/10.3390/cryst14121100/s1, Figure S1: DSC curve of MIT sample; Figure S2: Repeat DSC curve of MIT sample; Figure S3: The molecular structure of MIT; Figure S4: Crystal faces and unit cell determination/refinement of MIT; Table S1: Bond lengths [Å] and angles [°] of MIT; Figure S5: Histogram of prevalence of C-S-N angle ranges for acyclic sulfenamide structures in the CSD; Figure S6: ATR-FT-IR spectra of MIT with trace water; Table S2: Coordinates from DFT structure optimization of MIT; Figure S7: DFT calculated IR spectrum of MIT; Table S3: Input and coordinates of solid-state DFT structure of MIT using CRYSTAL17; Table S4: Input and coordinates of solid-state DFT structure of MCI using CRYSTAL17; Figure S8: Energy framework diagrams for

MIT calculated with CrystalExplorer; Table S5: Interaction energies calculated with CrystalExplorer. Reference [46] is cited in the Supplementary Materials.

Author Contributions: Conceptualization, R.G.; methodology, R.G. and N.N.; validation, R.G. and R.W.S.; formal analysis, R.G., N.N., R.W.S. and M.P.; investigation, R.G., M.P. and N.N.; resources, R.G.; data curation, R.G.; writing—original draft preparation, R.G., N.N. and R.W.S.; writing—review and editing, N.N.; visualization, R.G. and N.N.; supervision, N.N.; project administration, N.N. and R.G. All authors have read and agreed to the published version of the manuscript.

Funding: Open access was funded by the Max Planck Digital Library (MPDL).

Data Availability Statement: CCDC 2402883 contains the supplementary crystallographic data for this paper. The data can be obtained free of charge from the Cambridge Crystallographic Data Centre via www.ccdc.cam.ac.uk/structures.

Acknowledgments: We would like to thank Christian W. Lehmann and the board of directors of the Max-Planck-Institut für Kohlenforschung for providing laboratory resources. We would also like to thank Matthias Epple and Aileen Winter from the University of Duisburg-Essen for their help with the DSC measurements.

Conflicts of Interest: The authors declare no conflicts of interest.

References

1. Morley, J.O.; Oliver Kapur, A.J.; Charlton, M.H. Structure–activity relationships in 3-isothiazolones. *Org. Biomol. Chem.* **2005**, *3*, 3713–3719. [CrossRef] [PubMed]
2. Lundov, M.D.; Johansen, J.D.; Zachariae, C.; Moesby, L. Low-level efficacy of cosmetic preservatives. *Int. J. Cosmet. Sci.* **2011**, *33*, 190–196. [CrossRef] [PubMed]
3. Collier, P.J.; Ramsey, A.J.; Austin, P.; Gilbert, P. Growth inhibitory and biocidal activity of some isothiazolone biocides. *J. Appl. Bacteriol.* **1990**, *69*, 569–577. [CrossRef]
4. Wisastra, R.; Ghizzoni, M.; Maarsingh, H.; Minnaard, A.J.; Haisma, H.J.; Dekker, F.J. Isothiazolones; thiol-reactive inhibitors of cysteine protease cathepsin B and histone acetyltransferase PCAF. *Org. Biomol. Chem.* **2011**, *9*, 1817–1822. [CrossRef] [PubMed]
5. Crow, W.D.; Leonard, N.J. 3-Isothiazolone-cis-3-Thiocyanoacrylamide Equilibria1,2. *J. Org. Chem.* **1965**, *30*, 2660–2665. [CrossRef]
6. Silva, V.; Silva, C.; Soares, P.; Garrido, E.M.; Borges, F.; Garrido, J. Isothiazolinone Biocides: Chemistry, Biological, and Toxicity Profiles. *Molecules* **2020**, *25*, 991. [CrossRef] [PubMed]
7. Song, M.-K.; Baek, Y.-W.; Kim, D.I.; Yoon, S.-H.; Lee, K. Effects of stabilizer magnesium nirate on CMIT/MIT-induced respiratory toxicity. *Toxicol. Res.* **2023**, *39*, 373–382. [CrossRef] [PubMed]
8. Reinhard, E.; Waeber, R.; Niederer, M.; Maurer, T.; Maly, P.; Scherer, S. Preservation of products with MCI/MI in Switzerland. *Contact Dermat.* **2001**, *45*, 257–264. [CrossRef]
9. Ghose, A.K.; Viswanadhan, V.N.; Wendoloski, J.J. Prediction of Hydrophobic (Lipophilic) Properties of Small Organic Molecules Using Fragmental Methods: An Analysis of ALOGP and CLOGP Methods. *J. Phys. Chem. A* **1998**, *102*, 3762–3772. [CrossRef]
10. Alvarez-Sánchez, R.; Basketter, D.; Pease, C.; Lepoittevin, J.-P. Studies of Chemical Selectivity of Hapten, Reactivity, and Skin Sensitization Potency. 3. Synthesis and Studies on the Reactivity toward Model Nucleophiles of the ^{13}C-Labeled Skin Sensitizers, 5-Chloro-2-methylisothiazol-3-one (MCI) and 2-Methylisothiazol-3-one (MI). *Chem. Res. Toxicol.* **2003**, *16*, 627–636.
11. Arning, J.; Matzke, M.; Stolte, S.; Nehen, F.; Bottin-Weber, U.; Böschen, A.; Abdulkarim, S.; Jastorff, B.; Ranke, J. Analyzing Cytotoxic Effects of Selected Isothiazol-3-one Biocides Using the Toxic Ratio Concept and Structure−Activity Relationship Considerations. *Chem. Res. Toxicol.* **2009**, *22*, 1954–1961. [CrossRef] [PubMed]
12. Hunziker, N. The 'Isothiazolinone Story'. *Dermatology* **2009**, *184*, 85–86. [CrossRef]
13. Isaksson, M. Successful inhibition of allergic contact dermatitis caused by methylchloroisothiazolinone/methylisothiazolinone with topical glutathione. *Contact Dermat.* **2015**, *73*, 126–128. [CrossRef] [PubMed]
14. Gruvberger, B.; Bruze, M. Can Glutathione-Containing Emollients Inactivate methylchloroisothiazolinone/methylisothiazolinone? *Contact Dermat.* **1998**, *38*, 261–265. [CrossRef] [PubMed]
15. Crow, W.D.; Leonard, N.J. A synthesis of 3-isothiazolones. *Tetrahedron Lett.* **1964**, *5*, 1477–1480. [CrossRef]
16. Leonard, N.J.; Edwin Wilson, G. Rearrangement of a 1,4-thiazepine ring and formation of 3-isothiazolones. *Tetrahedron Lett.* **1964**, *5*, 1471–1475. [CrossRef]
17. Rothe, H.; Ryan, C.A.; Page, L.; Vinall, J.; Goebel, C.; Scheffler, H.; Toner, F.; Roper, C.; Kern, P.S. Application of in vitro skin penetration measurements to confirm and refine the quantitative skin sensitization risk assessment of methylisothiazolinone. *Regul. Toxicol. Pharmacol.* **2017**, *91*, 197–207. [CrossRef] [PubMed]
18. Virgilio, J.A.; Manowitz, M.; Heilweil, E. 2-Alkyl-3-Haloisothiazolium Salts and Their Derivatives 1979. U.S. Patent 4,281,136, 27 July 1981.
19. Sheldrick, G.M. SHELXT—Integrated space-group and crystal-structure determination. *Acta Crystallogr. A* **2015**, *71*, 3–8. [CrossRef]

20. Sheldrick, G.M. Crystal structure refinement with SHELXL. *Acta Crystallogr. C* **2015**, *71*, 3–8. [CrossRef] [PubMed]
21. Kleemiss, F.; Dolomanov, O.V.; Bodensteiner, M.; Peyerimhoff, N.; Midgley, L.; Bourhis, L.J.; Genoni, A.; Malaspina, L.A.; Jayatilaka, D.; Spencer, J.L.; et al. Accurate crystal structures and chemical properties from NoSpherA2. *Chem. Sci.* **2021**, *12*, 1675–1692. [CrossRef]
22. Midgley, L.; Bourhis, L.J.; Dolomanov, O.V.; Grabowsky, S.; Kleemiss, F.; Puschmann, H.; Peyerimhoff, N. Vanishing of the atomic form factor derivatives in non-spherical structural refinement—A key approximation scrutinized in the case of Hirshfeld atom refinement. *Acta Crystallogr. A* **2021**, *77*, 519–533. [CrossRef] [PubMed]
23. Bourhis, L.J.; Dolomanov, O.V.; Gildea, R.J.; Howard, J.A.K.; Puschmann, H. The anatomy of a comprehensive constrained, restrained refinement program for the modern computing environment—Olex2 dissected. *Acta Crystallogr. A* **2015**, *71*, 59–75. [CrossRef]
24. Neese, F. A perspective on the future of quantum chemical software: The example of the ORCA program package. *Faraday Discuss.* **2024**, *254*, 295–314. [CrossRef]
25. Becke, A.D. Density-functional thermochemistry. III. The role of exact exchange. *J. Chem. Phys.* **1993**, *98*, 5648–5652. [CrossRef]
26. Lee, C.; Yang, W.; Parr, R.G. Development of the Colle-Salvetti correlation-energy formula into a functional of the electron density. *Phys. Rev. B* **1988**, *37*, 785–789. [CrossRef] [PubMed]
27. Weigend, F.; Ahlrichs, R. Balanced basis sets of split valence, triple zeta valence and quadruple zeta valence quality for H to Rn: Design and assessment of accuracy. *Phys. Chem. Chem. Phys.* **2005**, *7*, 3297–3305. [CrossRef]
28. Macrae, C.F.; Sovago, I.; Cottrell, S.J.; Galek, P.T.A.; McCabe, P.; Pidcock, E.; Platings, M.; Shields, G.P.; Stevens, J.S.; Towler, M.; et al. Mercury 4.0: From visualization to analysis, design and prediction. *J. Appl. Crystallogr.* **2020**, *53*, 226–235. [CrossRef] [PubMed]
29. Spackman, P.R.; Turner, M.J.; McKinnon, J.J.; Wolff, S.K.; Grimwood, D.J.; Jayatilaka, D.; Spackman, M.A. CrystalExplorer: A program for Hirshfeld surface analysis, visualization and quantitative analysis of molecular crystals. *J. Appl. Crystallogr.* **2021**, *54*, 1006–1011. [CrossRef] [PubMed]
30. Hertwig, R.H.; Koch, W. On the parameterization of the local correlation functional. What is Becke-3-LYP? *Chem. Phys. Lett.* **1997**, *268*, 345–351. [CrossRef]
31. Weigend, F. Accurate Coulomb-fitting basis sets for H to Rn. *Phys. Chem. Chem. Phys.* **2006**, *8*, 1057–1065. [CrossRef]
32. Fletcher, R. *Practical Methods of Optimization*, 2nd ed.; John Wiley & Sons: Hoboken, NJ, USA, 2000.
33. Dovesi, R.; Erba, A.; Orlando, R.; Zicovich-Wilson, C.M.; Civalleri, B.; Maschio, L.; Rérat, M.; Casassa, S.; Baima, J.; Salustro, S.; et al. Quantum-mechanical condensed matter simulations with CRYSTAL. *WIREs Comput. Mol. Sci.* **2018**, *8*, e1360. [CrossRef]
34. Dovesi, R.; Pascale, F.; Civalleri, B.; Doll, K.; Harrison, N.M.; Bush, I.; D'Arco, P.; Noël, Y.; Rérat, M.; Carbonnière, P.; et al. The CRYSTAL code, 1976–2020 and beyond, a long story. *J. Chem. Phys.* **2020**, *152*, 204111. [CrossRef] [PubMed]
35. Bursch, M.; Mewes, J.-M.; Hansen, A.; Grimme, S. Best-Practice DFT Protocols for Basic Molecular Computational Chemistry. *Angew. Chem. Int. Ed.* **2022**, *61*, e202205735. [CrossRef] [PubMed]
36. Perdew, J.P.; Burke, K.; Ernzerhof, M. Generalized Gradient Approximation Made Simple. *Phys. Rev. Lett.* **1996**, *77*, 3865–3868. [CrossRef]
37. Grimme, S.; Ehrlich, S.; Goerigk, L. Effect of the damping function in dispersion corrected density functional theory. *J. Comput. Chem.* **2011**, *32*, 1456–1465. [CrossRef] [PubMed]
38. Grimme, S.; Hansen, A.; Brandenburg, J.G.; Bannwarth, C. Dispersion-Corrected Mean-Field Electronic Structure Methods. *Chem. Rev.* **2016**, *116*, 5105–5154. [CrossRef] [PubMed]
39. Grimme, S.; Antony, J.; Ehrlich, S.; Krieg, H. A consistent and accurate ab initio parametrization of density functional dispersion correction (DFT-D) for the 94 elements H-Pu. *J. Chem. Phys.* **2010**, *132*, 154104. [CrossRef]
40. Groom, C.R.; Bruno, I.J.; Lightfoot, M.P.; Ward, S.C. The Cambridge Structural Database. *Acta Crystallogr. Sect. B* **2016**, *72*, 171–179. [CrossRef]
41. Kato, M.; Fujihara, T.; Yano, D.; Nagasawa, A. 5-Chloro-2-methylisothiazolin-3-one: Intermolecular two-dimensional networks via unusual C-Cl...O&z-dbnd;C interactions. *Acta Crystallogr. Sect. E* **2007**, *63*, o3097.
42. Sekine, A.; Mitsumori, T.; Uekusa, H.; Ohashi, Y.; Yagi, M. Crystal Structure of a Host-guest Complex of Gallic Acid Methyl Ester and 5-Chloro-2-methyl-4-isothiazoline-3-one. *Anal. Sci. X-Ray Struct. Anal. Online* **2003**, *19*, x47–x48. [CrossRef]
43. Sekine, A.; Jomoto, K.; Uekusa, H.; Ohashi, Y.; Yagi, M. Crystal Structure of a Host-guest Complex of 4,4′-Ethylidenebisphenol and 5-Chloro-2-methyl-4-isothiazoline-3-one. *Anal. Sci. X-Ray Struct. Anal. Online* **2003**, *19*, x45–x46. [CrossRef]
44. Wang, F.; Chen, C.; Deng, G.; Xi, C. Concise Approach to Benzisothiazol-3(2H)-one via Copper-Catalyzed Tandem Reaction of o-Bromobenzamide and Potassium Thiocyanate in Water. *J. Org. Chem.* **2012**, *77*, 4148–4151. [CrossRef] [PubMed]
45. Kitaigorodsky, A.I. *Molecular Crystals and Molecules*; Academic Press: New York, NY, USA, 1973.
46. Mackenzie, C.F.; Spackman, P.R.; Jayatilaka, D.; Spackman, M.A. CrystalExplorer model energies and energy frameworks: Extension to metal coordination compounds, organic salts, solvates and open-shell systems IUCrJ 2017, 4, 575–587. *IUCrJ* **2017**, *4*, 575–587. [CrossRef] [PubMed]